PHILOSOPHICAL TRANSACTIONS A

royalsocietypublishing.org/journal/rsta

Research

Cite this article: Lo ACY, Bai J, Gladding PA, Fedorov VV, Zhao J. 2020 Afterdepolarizations and abnormal calcium handling in atrial myocytes with modulated SERCA uptake: a sensitivity analysis of calcium handling channels. *Phil. Trans. R. Soc. A* **378**: 20190557. http://dx.doi.org/10.1098/rsta.2019.0557

Accepted: 23 April 2020

One contribution of 16 to a theme issue 'Uncertainty quantification in cardiac and cardiovascular modelling and simulation'.

Subject Areas:
biomedical engineering

Keywords:
SERCA uptake, delayed afterdepolarizations, spontaneous depolarizations, altered calcium handling, bifurcation analysis, atrial fibrillation

Author for correspondence:
Jichao Zhao
e-mail: j.zhao@auckland.ac.nz

Electronic supplementary material is available online at https://doi.org/10.6084/m9.figshare.c.4979852.

THE ROYAL SOCIETY PUBLISHING

Afterdepolarizations and abnormal calcium handling in atrial myocytes with modulated SERCA uptake: a sensitivity analysis of calcium handling channels

Andy C. Y. Lo[1], Jieyun Bai[1,2], Patrick A. Gladding[3], Vadim V. Fedorov[4] and Jichao Zhao[1]

[1]Auckland Bioengineering Institute, The University of Auckland, Auckland, New Zealand
[2]Department of Electronic Engineering, College of Information Science and Technology, Jinan University, Guangzhou, People's Republic of China
[3]Department of Cardiology, Waitemata District Health Board, Auckland, New Zealand
[4]Department of Physiology and Cell Biology and Bob and Corrine Frick Center for Heart Failure and Arrhythmia, The Ohio State University Wexner Medical Center, Columbus, OH, USA

JZ, 0000-0003-3303-0401

Delayed afterdepolarizations (DADs) and spontaneous depolarizations (SDs) are typically triggered by spontaneous diastolic Ca^{2+} release from the sarcoplasmic reticulum (SR) which is caused by an elevated SR Ca^{2+}-ATPase (SERCA) uptake and dysfunctional ryanodine receptors. However, recent studies on the T-box transcription factor gene (TBX5) demonstrated that abnormal depolarizations could occur despite a reduced SERCA uptake. Similar findings have also been reported in experimental or clinical studies of diabetes and heart failure. To investigate the sensitivity of SERCA in the genesis of DADs/SDs as well as its dependence on other Ca^{2+} handling channels, we performed systematic analyses using the Maleckar *et al*. model. Results

showed that the modulation of SERCA alone cannot trigger abnormal depolarizations, but can instead affect the interdependency of other Ca^{2+} handling channels in triggering DADs/SDs. Furthermore, we discovered the existence of a threshold value for the intracellular concentration of Ca^{2+} ($[Ca^{2+}]_i$) for abnormal depolarizations, which is modulated by the maximum SERCA uptake and the concentration of Ca^{2+} in the uptake and release compartments in the SR ($[Ca^{2+}]_{up}$ and $[Ca^{2+}]_{rel}$). For the first time, our modelling study reconciles different mechanisms of abnormal depolarizations in the setting of 'lone' AF, reduced TBX5, diabetes and heart failure, and may lead to more targeted treatment for these patients.

This article is part of the theme issue 'Uncertainty quantification in cardiac and cardiovascular modelling and simulation'.

1. Introduction

Atrial fibrillation (AF) leads to the rapid and irregular contraction of the upper chambers of the heart, characterized by the disorganized electrical activity within the atria [1]. It is the most encountered arrhythmia in clinical practice, and if left untreated, can lead to an increased risk of heart failure, stroke, and mortality [2]. AF is associated with an increased risk from conditions such as diabetes, obesity, and hypertension [3,4] or from old age [5]. Altered Ca^{2+} homeostasis is strongly implicated in the initiation of AF [6,7]. In paroxysmal AF, self-terminating episodes of arrhythmia occur in structurally normal atria. This has been linked with increased diastolic Ca^{2+} leak from the sarcoplasmic reticulum (SR) and triggered activity from upregulated SR Ca^{2+} ATPase2a (SERCA) and type 2 ryanodine receptor (RyR) dysregulation [7–10]. Similarly, an elevated SERCA uptake was observed in patients with persistent AF [10].

Recent studies from referral populations and in the community suggest that the familial clustering of AF may be genetically caused [11–15]. Furthermore, epidemiological studies have found that individuals who have a first-degree relative with lone AF carry an eightfold increased risk of AF [16]. Linkage and candidate gene sequencing methods have identified several rare genetic variants in genes encoding proteins which alter the kinetics of ion channels, leading to AF [17,18]. With the advent of the genome-wide association studies (GWAS) approach, studies were instead predominantly focused on identifying the common genetic variants associated with AF in the general population [19].

Among recent large-scale GWAS studies, multiple transcription factor genes including the T-box transcription factor gene TBX5 were found to be strongly associated with the arrhythmia [20–24]. TBX5 is known primarily for its role in cardiac development and rhythm control during embryogenesis [25]. Mutations in TBX5 have been reported to underlie Holt-Oram syndrome, features of which include conduction abnormalities and AF [26]. Through a crucial knockout mice study by Nadadur *et al*. [27], they demonstrated that impairment in TBX5 expression resulted in delayed afterdepolarizations (DADs) and spontaneous depolarizations (SDs) which can lead to AF (figure 1*a*) [28]. Dai *et al*. hypothesized that these abnormalities were caused by the remodelling of Ca^{2+} handling channels and they conducted a subsequent study to investigate their activity in TBX5 knockout mice [29]. Using an experimental protocol with caffeine-containing, Na^+-free, Tyrode solution to block Ca^{2+} extrusion through I_{NaCa}, and then a protocol with Na^+ containing caffeine solution to prevent uptake through SERCA in the subsequent experiment, they found that the activity of SERCA and I_{NaCa} had decreased and increased respectively. The conductivity of the L-type Ca^{2+} current (I_{CaL}) was also shown to have increased through a voltage-clamp experiment. In addition, they found that if the SERCA inhibitor phospholamban (PLN) was reduced in these TBX5 knockout atrial myocytes, then this instead restored SERCA activity and abolished DADs/SDs. This is intriguing, as these DADs and SDs were caused by a reduction in SERCA instead.

In relation to this, experimental studies on heart failure and diabetes have also reported a reduction in SERCA and an increase in I_{NaCa} [6,30–33], as well as the elevated occurrence

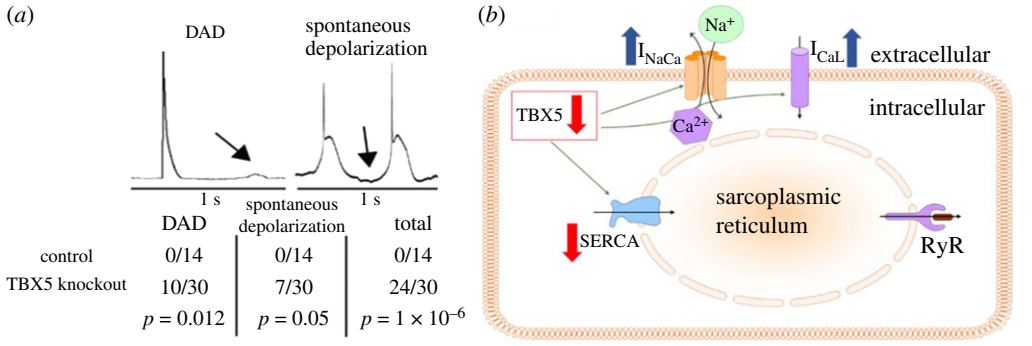

Figure 1. (*a*) Example of experimental traces of the membrane potential from the experiment by Nadadur *et al*. [27]. Delayed afterdepolarizations (DADs) and spontaneous depolarizations (SDs) occur for a majority of (homogeneous TBX5 knockout) mice atrial myocytes, but none for control mice atrial myocytes. (*b*) Simplified schematic highlighting that reduced expression of TBX5 reduces sarcoplasmic reticulum Ca^{2+} ATPase 2a (SERCA) and increases I_{NaCa} and I_{CaL}, respectively. (Online version in colour.)

of DADs/SDs [34,35]. Furthermore, restoration of SERCA function through viral transfection of SERCA into cardiac tissue *in vivo* or knockout of PLN has also been shown to improve cardiomyocyte contractility and suppress triggered activities in both animal and clinical studies of heart failure and diabetes [36–39]. Together, these studies highlight our incomplete understanding of the sensitivity of SERCA in DAD/SD genesis as well as its dependence on other key Ca^{2+} handling channels such as the RyR, I_{NaCa}, and I_{CaL}.

There has also been much debate into the actual mechanisms by which spontaneous diastolic Ca^{2+} release from the SR can occur to trigger DADs/SDs [40]. Several reports have hypothesized that this is due to the overload of Ca^{2+} in the SR, termed store-overload induced Ca^{2+} release [41–43]. Some experimental studies have instead indicated that a more loaded SR is not the only prerequisite for spontaneous diastolic Ca^{2+} release [44]. Using heart failure as an example, there have been reports that DADs/SDs can appear during this condition despite low Ca^{2+} levels in the SR [33,45–47].

Altered Ca^{2+} handling and its implications on the mechanisms of triggered activity can only be explored through a computer model as it is a powerful tool for quantitative dissection of the fundamental mechanisms and in investigating their individual role in DADs/SDs [48]. In this study, we use the Maleckar *et al*. model [49] to explore the complex relationship between SERCA and other Ca^{2+} handling channels, and how changes in this relationship affect the Ca^{2+} dynamics and the susceptibility of the atrial myocyte to DADs/SDs. We define an SD as a self-depolarization that has reached -50 mV or higher, and a DAD as a self-depolarization that is below −50 mV. Throughout this study, we consider only the occurrence of SDs in our results as it is easier to identify in simulation than DADs. However, all our analysis and results for SDs are applicable to DADs as well.

2. Methods

(a) The Maleckar *et al*. model

The Maleckar *et al*. model was based on the human atrial myocyte model of Nygren *et al*. [50,51], and was designed to accurately capture the repolarization phase of an action potential (AP) at different cycle lengths [49,52]. In the Maleckar *et al*. model (figure 2), the time and voltage-dependent currents I_{Na} (Na^+ current), I_{CaL}, I_t, I_{Kur}, I_{K1}, I_{Kr}, and I_{Ks} (Ca^{2+} independent transient outward, ultra-rapid, inward rectifier and delayed rectifier K^+ currents, respectively) are the main attributors to the generation of the human atrial AP.

Ca^{2+} cycling occurs through SERCA and RyR, located on the SR. The uptake of Ca^{2+} from the intracellular domain follows a bidirectional formulation [53], where if the concentration of Ca^{2+}

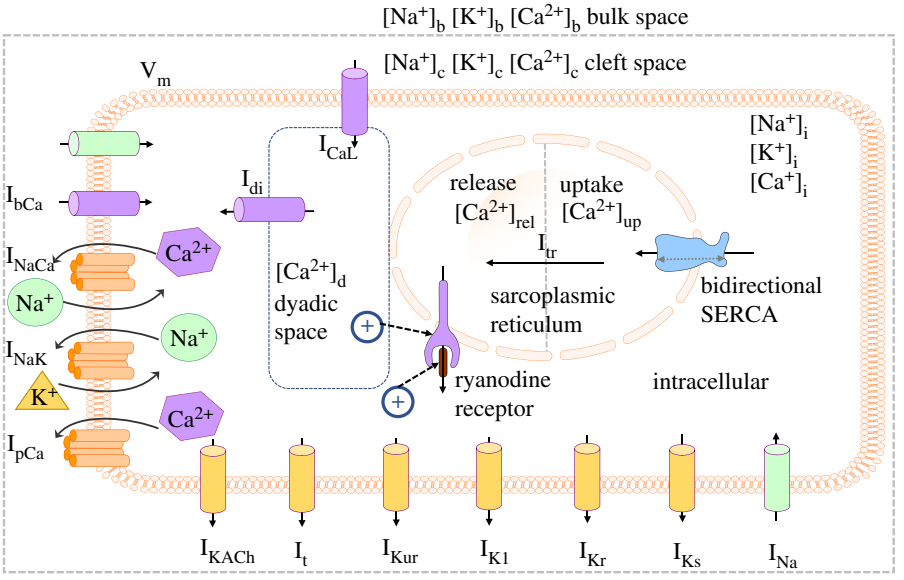

Figure 2. Schematic of the full Maleckar *et al.* model [49]. The sarcoplasmic reticulum Ca^{2+} ATPase2a (SERCA) pump is bidirectional, and the activation of the ryanodine receptor is modulated by $[Ca^{2+}]_d$ and $[Ca^{2+}]_i$. (Online version in colour.)

in the uptake compartment ($[Ca^{2+}]_{up}$) becomes high relative to the concentration of Ca^{2+} in the intracellular ($[Ca^{2+}]_i$), then the pump will operate more prominently in the reverse direction to reduce the net flux from SERCA. In addition, Ca^{2+} is transferred from the uptake compartment to the release compartment through I_{tr} (transfer current). Activation of the RyR is modulated by the concentration of Ca^{2+} in the dyadic space and intracellular ($[Ca^{2+}]_d$ and $[Ca^{2+}]_i$, respectively). Release of Ca^{2+} from the SR is triggered when $[Ca^{2+}]_d$ and/or $[Ca^{2+}]_i$ is sufficiently elevated, known as Ca^{2+}-induced Ca^{2+} release. Once activated, the concentration difference between $[Ca^{2+}]_{rel}$ and $[Ca^{2+}]_i$ determines the magnitude of I_{rel}.

Currently, the only reported functional changes due to a reduction in TBX5 are from experimental studies by Dai *et al.* [29] and Laforest *et al.* [54]. Voltage-clamp experiments show an increase in I_{CaL} in atrial myocytes with reduced expression of TBX5, and separate caffeine-based protocols demonstrated a reduction in SERCA and an elevation in I_{NaCa} activity through measurements in the decay rate of $[Ca^{2+}]_i$. Similar findings have also been reported in the setting of diabetes and heart failure [32,35,38,55]. Hence, we model functional changes in SERCA as simply a multiplicative change in maximum SERCA uptake, and changes in I_{CaL} and I_{NaCa} as a change in their conductivity. In addition, because the underlying commonality behind these conditions is disrupted Ca^{2+} handling, we have also included RyR in this study, and changes in its activity will also be modelled as a change in its conductivity. The study will be carried out across a wide parameter space to assess how changes in these parameters impact Ca^{2+} handling.

Throughout our experiments, we define the control as the original full Maleckar *et al.* model with its original parameters and equations, i.e. normal human atrial myocytes under physiological conditions. In each of our simulations with the full cellular model, a train of stimuli with a duration of 6 ms and magnitude of −15 pA/pF was applied at a frequency of 1 Hz up to 100 s into the simulation.

(b) Bifurcation analysis and sensitivity of SERCA

We first investigated how the individual sensitivity of SERCA compared with that of I_{CaL}, I_{NaCa}, and RyR in the genesis of SDs by running simulations where we individually varied the conductivities of these channels from a range of 0 to 2 times its control value. We then probed for

the minimum increase or decrease required for each channel for an SD to occur in increments of 0.01 until it was identified.

Afterwards, we conducted a type of analysis known as a bifurcation analysis to investigate how changes in the parameter of a Ca^{2+} handling channel affected that of another channel in triggering SDs. The first bifurcation analysis we performed was between I_{CaL} and I_{NaCa} with SERCA at its control value. We varied the conductivity of I_{CaL} from a range of 0.2 to 2 times its control value in increments of 0.2, and for each of these values of I_{CaL}, we identified the minimum multiplier that must be applied to I_{NaCa} to trigger at least one SD. Following this, we then conducted three other bifurcation analyses and identified minimum multipliers for RyR, I_{CaL}, and I_{NaCa} for varying levels of SERCA using the same approach.

Minimum multipliers were determined through a trial and error approach. For example, if we were interested in finding the minimum multiplier that must be applied to RyR to trigger at least one SD, then we ran simulations of the full Maleckar *et al*. model with SERCA set at a certain condition, e.g. 120% of its original value, for varying levels of RyR until we ascertain a rough estimate of the parameter region where the SDs occur. After this, we honed in onto the minimum multiplier value for RyR that could cause at least one SD to occur for 120% SERCA. Through this approach, we derived the SD boundary lines for each of the corresponding bifurcation diagrams which illustrated the relationship between Ca^{2+} handling parameter pairs in the genesis of at least one SD.

(c) Calcium subsystem analysis

In the full Maleckar *et al*. model, it can be quite complex to identify the exact mechanisms to trigger an SD since many factors can influence this. However, by reducing the model down to only the essentials in Ca^{2+} handling, i.e. Ca^{2+} subsystem (electronic supplementary material, figure S1), we can instead probe for the conditions for Ca^{2+} oscillations instead which is far simpler to identify as they only take place when the myocyte is overloaded with Ca^{2+}. These conditions can then be applied to the full Maleckar *et al*. model to investigate the mechanisms of SDs as such abnormal depolarizations are triggered by the occurrence of Ca^{2+} oscillations in the Ca^{2+} subsystem [56–60]. To carry out this Ca^{2+} subsystem analysis, we used the approach developed by Fink *et al*. [40].

To reduce the Maleckar *et al*. model down to its Ca^{2+} subsystem, we set all transmembrane currents apart from I_{NaCa} to zero, and set the membrane potential and intracellular and cleft space Na^{+} concentrations to a constant value as determined by their end-diastolic values after 3000 s of 1 Hz pacing in the full Maleckar *et al*. model. Note that I_{CaL} was also removed despite playing an important role in Ca^{2+} handling in the full model because since the membrane potential was clamped, I_{CaL} would not activate, and hence would provide a negligible amount of Ca^{2+} into the reduced model. Since the bulk space and K^{+} concentrations were not required in the Ca^{2+} subsystem, we removed them from the reduced model (electronic supplementary material, figure S1).

To induce an overload of Ca^{2+}, a multiplier was applied to clamped $[Na^{+}]_i$. This multiplier caused a rise in Ca^{2+} in the myocyte, which triggered I_{NaCa} to extrude Na^{+} out of the cell and Ca^{2+} into the cell. A minimum multiplier was required to sufficiently elevate the total Ca^{2+} in the myocyte (which we defined as $[Ca^{2+}]_{tot} = [Ca^{2+}]_{up} + [Ca^{2+}]_{rel} + [Ca^{2+}]_{d} + [Ca^{2+}]_{i)}$ so that Ca^{2+} oscillations occurred. During this phenomenon, $[Ca^{2+}]_{up}$, $[Ca^{2+}]_{rel}$, $[Ca^{2+}]_{d}$, and $[Ca^{2+}]_{i}$ oscillated between a maximum and minimum value as time progressed. These oscillations would persist since $[Na^{+}]_i$ remained fixed at that elevated value.

We considered the system as having successfully generated Ca^{2+} oscillations if the average range during the simulation time-course of 5000 s was at least 0.2 mM for $[Ca^{2+}]_{up}$, $[Ca^{2+}]_{rel}$, and 0.00002 mM for $[Ca^{2+}]_{d}$, and $[Ca^{2+}]_{i}$. Note that if the multiplier for $[Na^{+}]_i$ could not sufficiently elevate $[Ca^{2+}]_{tot}$ to trigger SDs, then $[Ca^{2+}]_{up}$, $[Ca^{2+}]_{rel}$, $[Ca^{2+}]_{d}$, and $[Ca^{2+}]_{i}$ would not oscillate and would immediately reach steady state instead.

Using the reduced model, we implemented the changes in SERCA, RyR, and I_{NaCa} from a range of 0.2 to 2 times their respective control values in increments of 0.2 individually. For each increase for a particular channel, we then found the minimum multiplier required for clamped $[Na^+]_i$ to subsequently elevate the total Ca^{2+} concentration in the atrial myocyte sufficiently to trigger Ca^{2+} oscillations. The corresponding minimum $[Ca^{2+}]_{tot}$ that triggered Ca^{2+} oscillations was derived by finding the steady state for $[Ca^{2+}]_{up}$, $[Ca^{2+}]_{rel}$, $[Ca^{2+}]_d$, and $[Ca^{2+}]_i$ during these oscillations. Steady state for each compartment was obtained by computing their mean value over the simulation time-course of 5000 s. This approach was then used to investigate how changes in the Ca^{2+} handling channels along the points on the SD boundary line for SERCA-RyR and SERCA-I_{NaCa} bifurcations impacted the minimum $[Ca^{2+}]_{tot}$ for Ca^{2+} oscillations and hence SDs.

(d) The dependency test of ryanodine receptors and SERCA on the genesis of spontaneous depolarizations

As previously mentioned, there is much debate in experimental studies regarding the precise mechanisms by which diastolic spontaneous Ca^{2+} release occurs to trigger SDs. However, in the study by Fink *et al*., the importance of the modulation of $[Ca^{2+}]_i$ and $[Ca^{2+}]_{up}$ on SERCA, and $[Ca^{2+}]_i$ and $[Ca^{2+}]_d$ on RyR in the genesis of SDs was also investigated.

We conducted this dependency test on the full Maleckar *et al*. model to determine the necessary properties for the initiation of SDs in this model. To carry this out, we first applied a train of stimuli with a duration of 6 ms and magnitude of -15 pA/pF at a frequency of 1 Hz up to 3000 s into the simulation. At 3000 s, we recorded the values of $[Ca^{2+}]_{up}$, $[Ca^{2+}]_i$, and $[Ca^{2+}]_d$, and labelled them as $[Ca^{2+}]_{up,3000s}$, $[Ca^{2+}]_{i,3000s}$, and $[Ca^{2+}]_{d,3000\,s,}$ respectively.

To illustrate the subsequent steps, we then used the RyR as an example, the modulation terms of the RyR in the full Maleckar *et al*. model were given by

$$r_{Ca_{d\,term}} = \frac{[Ca^{2+}]_d}{[Ca^{2+}]_d + k_{rel_d}}, \tag{2.1}$$

$$r_{Ca_{i\,term}} = \frac{[Ca^{2+}]_i}{[Ca^{2+}]_i + k_{rel_i}}, \tag{2.2}$$

$$r_{Ca_{d\,factor}} = (r_{Ca_{d\,term}})^3, \tag{2.3}$$

and

$$r_{Ca_{i\,factor}} = (r_{Ca_{i\,term}})^3. \tag{2.4}$$

To remove the modulation of $[Ca^{2+}]_i$ on RyR to test its dependence on the genesis of SDs, we substituted $[Ca^{2+}]_i$ in equation (2.2) with $[Ca^{2+}]_{i,3000s}$. This gave

$$r_{Ca_{i\,term}} = \frac{[Ca^{2+}]_{i,\,3000s}}{[Ca^{2+}]_{i,\,3000s} + k_{rel_i}}. \tag{2.5}$$

To test the dependence of $[Ca^{2+}]_d$ on RyR, we substituted $[Ca^{2+}]_d$ in equation (2.1) with $[Ca^{2+}]_{d,3000\,s}$. This gave

$$r_{Ca_d term} = \frac{[Ca^{2+}]_{d,\,3000s}}{[Ca^{2+}]_{d,\,3000s} + k_{rel\,d}}. \tag{2.6}$$

By a similar approach, the dependence of $[Ca^{2+}]_i$ and $[Ca^{2+}]_{up}$ on SERCA in the full Maleckar *et al*. model was also tested.

(e) Intracellular calcium injection protocols

The first protocol was designed to investigate the threshold value for $[Ca^{2+}]_i$ in triggering SDs, and whether this threshold followed a biphasic trend as SERCA decreased from 200% to 20% of its control value. The second protocol was designed to assess whether $[Ca^{2+}]_{up}$ and $[Ca^{2+}]_{rel}$ were also determining factors in $[Ca^{2+}]_i$ SD threshold for various levels of SERCA, and to ascertain

how changes in SERCA impacted Ca^{2+} handling and hence gave rise to the biphasic trend in the $[Ca^{2+}]_i$ SD threshold.

(i) Intracellular calcium injection protocol 1

We applied a train of stimuli with a duration of 6 ms, magnitude of −15 pA/pF and frequency of 1 Hz up to 100 s into the simulation. At exactly 100 s into the simulation, we recorded the value of $[Ca^{2+}]_i$, then applied a multiplier to this value. This new value was then used to replace the original value of $[Ca^{2+}]_i$, and the simulation was then resumed except no external stimulus was applied. This protocol was repeated until we found the minimum multiplier required to increase $[Ca^{2+}]_i$ to the threshold value needed to trigger an SD at 100 s. The protocol was performed for values of SERCA from 20% to 200% control SERCA in increments of 20%.

(ii) Intracellular calcium injection protocol 2

For this protocol, we followed the same steps as outlined above, except exactly 100 s into the simulation, we adjusted $[Ca^{2+}]_{up}$ and $[Ca^{2+}]_{rel}$ to their value at 20% SERCA at 100 s in protocol 1 before we applied the multiplier to $[Ca^{2+}]_i$. The same protocol in protocol 1 was repeated but with $[Ca^{2+}]_{up}$ and $[Ca^{2+}]_{rel}$ adjusted to their value at 200% at 100 s instead.

3. Results

(a) The impact of individual calcium handling channels on spontaneous depolarizations

From our series of simulations where we individually implemented the remodelling of each Ca^{2+} handling channel from a range of 0% to 200% of their control value, we identified a minimum value that I_{NaCa}, I_{CaL}, RyR, and SERCA must be increased or decreased to trigger SDs. For I_{NaCa}, SDs occurred when it was decreased by 11%, while for I_{CaL} and RyR, they instead occurred when they were increased by 13% and 38%, respectively (figure 3*a*). We were unable to identify a minimum value by which we needed to increase or decrease SERCA alone to generate SDs. In figure 3*b–f*, we show the time-course of the membrane potential, I_{rel}, $[Ca^{2+}]_i$, $[Ca^{2+}]_{up}$, and $[Ca^{2+}]_{rel}$ after the last stimulated AP (black triangle) and the SDs occurred at their respective minimum percentage for I_{NaCa}, I_{CaL}, and RyR.

(b) The sensitivity of spontaneous depolarizations to SERCA

We examined the relationship between I_{CaL} and I_{NaCa} in SDs through a bifurcation analysis (figure 4*a*). As shown by the blue SD boundary quadratic line in figure 4*a*, as we increased the multiplier to I_{CaL}, the minimum multiplier for I_{NaCa} required to generate SDs also increased. The region below the blue SD boundary line illustrates the parameter range between I_{CaL} and I_{NaCa} where SDs can occur.

We then chose a data point on the blue line of the I_{CaL}-I_{NaCa} bifurcation (figure 4*a*), e.g. $1.4 \times I_{CaL}$, $1.25 \times I_{NaCa}$, and ran a series of simulations where we changed SERCA from 0% to 200% of its control value to ascertain how changes in SERCA affected the capacity of I_{CaL}, and I_{NaCa} in generating SDs. As expected, SDs were observed when we kept SERCA at its control value with 140% I_{CaL} and 125% I_{NaCa} since we used a pair of values on the SD threshold of I_{CaL} and I_{NaCa}. However, SDs were abolished when SERCA was reduced below 55% or increased above 106% of its control value (figure 4*b*). This illustrates an interdependency between SERCA with I_{CaL} and I_{NaCa}, as SDs only occurred within a certain parameter range for SERCA. In figure 4*c–f*, we show the time-course of I_{rel}, $[Ca^{2+}]_i$, $[Ca^{2+}]_{up}$, and $[Ca^{2+}]_{rel}$ after the last stimulated AP with SERCA at 100%, 54%, 107% of its control value.

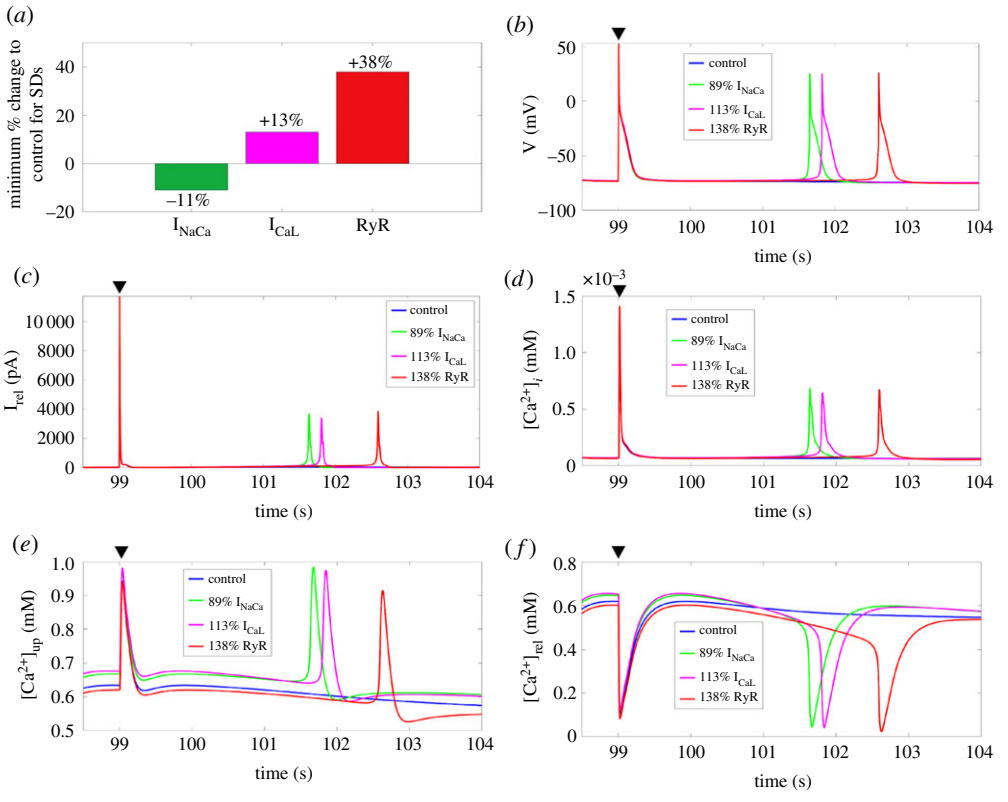

Figure 3. (*a*) The minimum percentage change to control individual I_{NaCa}, I_{CaL} and RyR to trigger SDs. (*b–f*) Time-course of the membrane potential, I_{rel}, $[Ca^{2+}]_i$, $[Ca^{2+}]_{up}$, and $[Ca^{2+}]_{rel}$, for control and for 89% I_{NaCa}, 113% I_{CaL}, and 138% RyR after the last stimulated AP (black triangle). SERCA, sarcoplasmic reticulum Ca^{2+}-ATPase; SD, spontaneous depolarization; RyR, ryanodine receptors. (Online version in colour.)

(c) Bifurcation analysis between SERCA and other calcium handling channels

As observed in the previous subsection, changes in SERCA can have an impact on I_{CaL}, RyR, and I_{NaCa} in generating SDs. To investigate this issue systematically, we conducted a SERCA-I_{CaL}, SERCA-RyR and SERCA-I_{NaCa} bifurcation. For both SERCA-RyR and SERCA-I_{CaL} bifurcations (figure 5*a*,*b*), at less than approximately 80% SERCA, the minimum multiplier for I_{CaL} and RyR required to generate at least an SD decreased linearly with increasing SERCA. However, at greater than approximately 80%, the minimum multiplier for I_{CaL} and RyR instead increased linearly with increasing SERCA. For the SERCA-I_{NaCa} bifurcation, at less than approximately 80% SERCA, the minimum multiplier for I_{NaCa} instead increased linearly with increasing SERCA, but decreased linearly at greater than approximately 80% (figure 5*c*). Together, this implied that at approximately 80% SERCA, there was a shift in the Ca^{2+} handling of the atrial myocyte since that was roughly the point where the trend changed direction for all three bifurcation diagrams.

(d) The calcium subsystem sensitivity analysis of SERCA

Under this subsection, we conducted a Ca^{2+} subsystem sensitivity analysis to investigate how changes in SERCA, RyR, and I_{NaCa} alone affected the minimum multiplier to clamped $[Na^+]_i$ (and hence the total Ca^{2+} concentration threshold) to generate Ca^{2+} oscillations. For either SERCA or I_{NaCa}, as it decreased from 200% of its control value to 40% of its control value, the minimum multiplier to clamped $[Na^+]_i$ also decreased (electronic supplementary material, figure S2). By

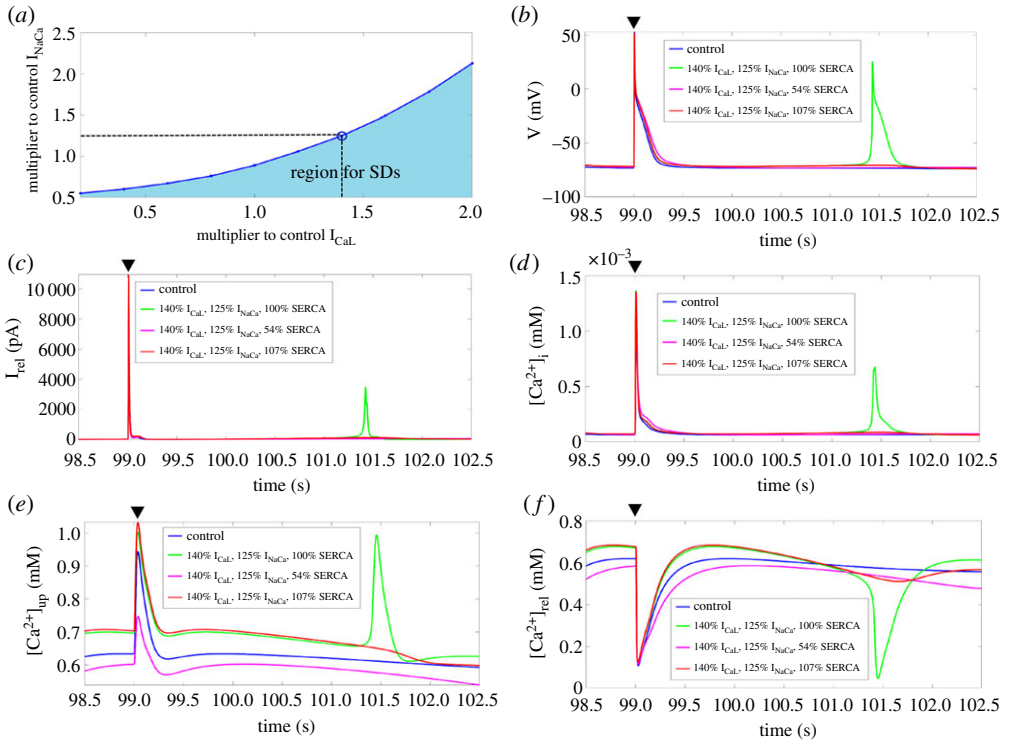

Figure 4. (*a*) Bifurcation diagram of I_{CaL} and I_{NaCa} at 100% SERCA. Shaded region illustrates the parameter range where SDs occur. (*b–f*) Time-course of the membrane potential, I_{rel}, $[Ca^{2+}]_i$, $[Ca^{2+}]_{up}$, and $[Ca^{2+}]_{rel}$ for control and at 140% I_{CaL} and 125% I_{NaCa} for 100%, 54%, and 107% SERCA after the last stimulated AP (black triangle). SERCA, sarcoplasmic reticulum Ca^{2+}-ATPase; SD, spontaneous depolarization; AP, action potential. (Online version in colour.)

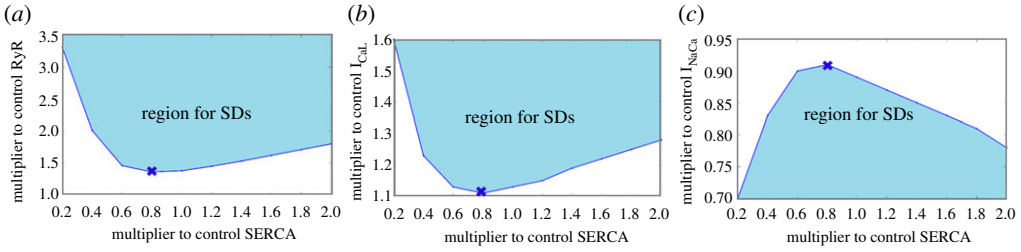

Figure 5. Bifurcation analysis for SERCA-RyR (*a*) and SERCA-I_{Cal} (*b*), respectively. (*c*) Bifurcation analysis for SERCA-I_{NaCa}. Shaded region illustrates the parameter range where SDs occur. The cross marks roughly where the shift in the Ca^{2+} handling took place. SERCA, sarcoplasmic reticulum Ca^{2+}-ATPase; SD, spontaneous depolarization; RyR, ryanodine receptors. (Online version in colour.)

contrast, the minimum multiplier to clamped $[Na^+]_i$ instead increased as RyR decreased. Since the existence of Ca^{2+} oscillations in the Ca^{2+} subsystem corresponded to the occurrence of SDs in the full model, this showed that reducing SERCA or I_{NaCa} alone decreased the minimum total Ca^{2+} concentration required for Ca^{2+} oscillations, while reducing RyR instead has the opposite effect.

We then conducted a subsequent analysis to find how changes along the SD boundary in the direction of increasing SERCA for both SERCA-RyR and SERCA-I_{NaCa} bifurcations affected the minimum multiplier for clamped $[Na^+]_i$ for Ca^{2+} oscillations to occur. The obtained data

points for the minimum multiplier for clamped $[Na^+]_i$ from the changes in SERCA and I_{NaCa}, and changes in SERCA and RyR along the SD boundary line in their respective bifurcation diagrams were then compared with the points obtained from changes in SERCA alone (electronic supplementary material, figure S2).

As shown in electronic supplementary material, figure S3A, as we went in the direction of decreasing SERCA, the minimum multiplier for clamped $[Na^+]_i$ for Ca^{2+} oscillations decreased for all three cases. Correspondingly, decreasing SERCA uptake function reduced the minimum $[Ca^{2+}]_{tot}$ needed for SDs to occur, and thus increased the myocyte's susceptibility to SDs in the full Maleckar *et al*. model (electronic supplementary material, figure S3B). Interestingly, electronic supplementary material, figure S3B also showed that only the minimum $[Ca^{2+}]_{tot}$ for SDs was significantly different for changes in both SERCA and RyR based upon the points in the SD boundary of the SERCA-RyR bifurcation. This, along with the linear decreasing tend among the three cases suggested that reducing the minimum $[Ca^{2+}]_{tot}$ was not the only requirement for SDs to occur, and that a deeper mechanism existed alongside this.

(e) The necessary components of the genesis of spontaneous depolarizations

One plausible explanation for the biphasic trend in the SERCA-RyR, SERCA-I_{CaL}, and SERCA-I_{NaCa} bifurcation diagrams was due to the Ca^{2+} threshold required to trigger SDs changing in a biphasic manner as SERCA changes, and thus different minimum increases in RyR and I_{CaL}, or decreases in I_{NaCa} were required to meet this Ca^{2+} threshold for various levels of SERCA. To be able to determine if this was the case, we first needed to identify the necessary components in the Maleckar *et al*. model to give rise to an SD. Hence we performed the dependency test proposed by Fink *et al*. where we tested the modulation of $[Ca^{2+}]_i$ and $[Ca^{2+}]_{up}$ on SERCA, and $[Ca^{2+}]_i$ and $[Ca^{2+}]_d$ on RyR to see which ones were essential for the genesis of SDs. Through this test, we found that only the modulation of RyR by $[Ca^{2+}]_i$ was crucial for the initiation of SDs (figure 6*b*).

(f) The impact of SERCA on the intracellular calcium threshold for spontaneous depolarizations

Having determined that it was the modulation of $[Ca^{2+}]_i$ on RyR that was essential in the genesis of SDs in the full Maleckar *et al*. model, we were then interested in ascertaining whether there existed a threshold value for $[Ca^{2+}]_i$ in triggering SDs, and whether this threshold followed a biphasic trend as SERCA decreased from 200% to 20% of its control value. Hence, we performed the intracellular Ca^{2+} injection protocol 1 for various levels of SERCA. As shown in figure 7, the $[Ca^{2+}]_i$ threshold to trigger SDs followed a biphasic trend as SERCA decreased from 200% to 20% of its control value, demonstrating that this threshold was different for varying levels of SERCA. This also confirmed that when SERCA was sufficiently inhibited or elevated, to trigger SDS, an increase in RyR, I_{CaL}, or decrease in I_{NaCa} was required to meet the elevated $[Ca^{2+}]_i$ threshold to trigger SDs.

(g) The relationship between calcium concentrations in the uptake and release compartment and the intracellular calcium threshold

Having confirmed that there existed a threshold value for $[Ca^{2+}]_i$ in triggering SDs and that the threshold followed a biphasic trend as SERCA decreased, we were then interested in knowing the Ca^{2+} handling mechanisms which gave rise to the biphasic relationship between the $[Ca^{2+}]_i$ SD threshold and SERCA. We hypothesized that this mechanism not only involved SERCA but also $[Ca^{2+}]_{up}$ and $[Ca^{2+}]_{rel}$, because as we were conducting the experiment under protocol 1, we noted that they kept decreasing as SERCA decreased (electronic supplementary material, figure S4A and B). Hence, there was the possibility that different levels in $[Ca^{2+}]_{up}$ and $[Ca^{2+}]_{rel}$ could therefore also have an impact on the $[Ca^{2+}]_i$ SD threshold.

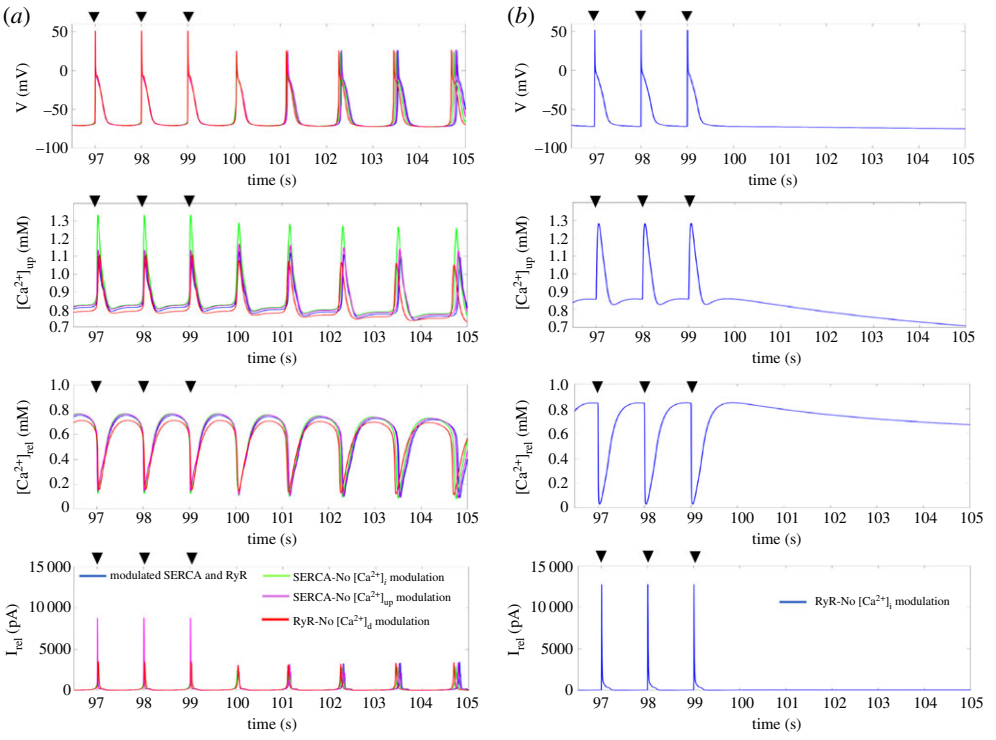

Figure 6. The dependency test of SERCA and RyR in the genesis of SDs. (*a*) Time-course of the membrane potential, $[Ca^{2+}]_{up}$, $[Ca^{2+}]_{rel}$, and I_{rel} for modulated SERCA and RyR, removed modulation of $[Ca^{2+}]_i$ on SERCA, removed modulation of $[Ca^{2+}]_{up}$ on SERCA, and removed modulation of $[Ca^{2+}]_d$ on RyR. (*b*) Time-course of the membrane potential, $[Ca^{2+}]_{up}$, $[Ca^{2+}]_{rel}$, and I_{rel} for removed modulation of $[Ca^{2+}]_i$ on RyR. The black triangle indicates the time when a stimulus was applied. SERCA, sarcoplasmic reticulum Ca^{2+}-ATPase; SD, spontaneous depolarization; RyR, ryanodine receptors. (Online version in colour.)

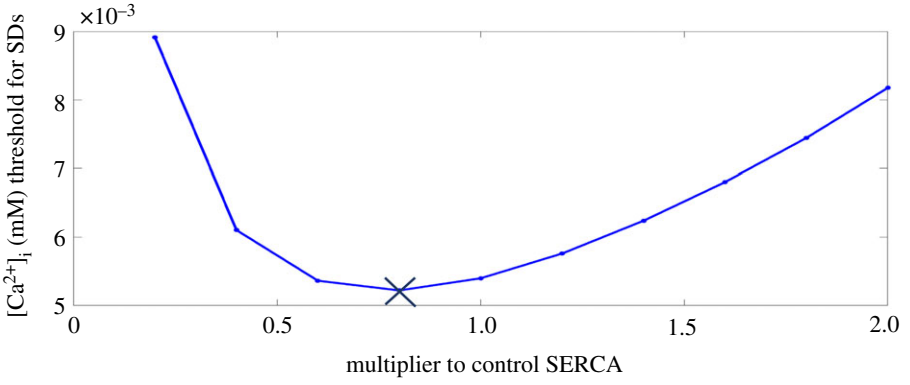

Figure 7. The $[Ca^{2+}]_i$ SD threshold for various levels of SERCA. The cross represents the point where the trend changed. SERCA, sarcoplasmic reticulum Ca^{2+}-ATPase. (Online version in colour.)

To investigate this, we conducted two more series of simulations under intracellular calcium injection protocol 2. These series of simulations respectively assessed how the $[Ca^{2+}]_i$ SD threshold was impacted when $[Ca^{2+}]_{up}$ and $[Ca^{2+}]_{rel}$ was reduced or increased beyond their intrinsic value for a particular level of SERCA. As shown in figure 8, when $[Ca^{2+}]_{rel}$ and $[Ca^{2+}]_{up}$

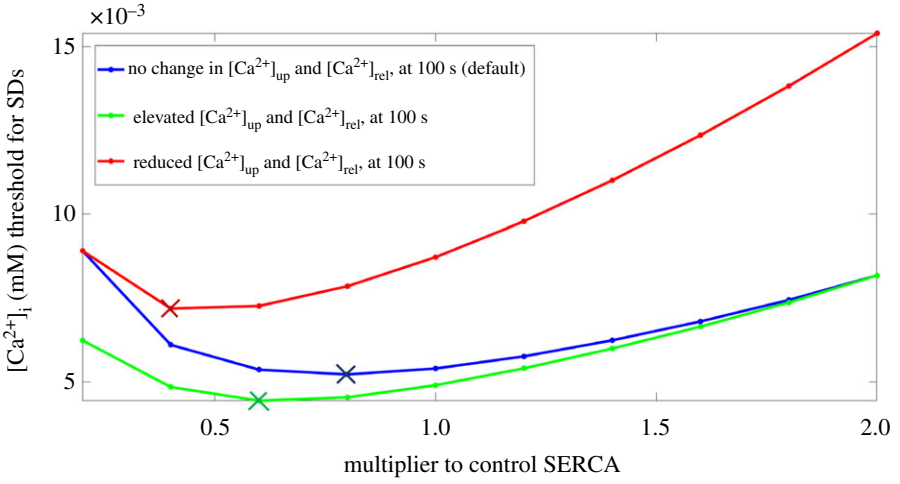

Figure 8. The $[Ca^{2+}]_i$ SD threshold for various levels of SERCA for three different cases. The default case is when no change was made to $[Ca^{2+}]_{up}$ and $[Ca^{2+}]_{rel}$ at 100 s into the simulation (blue). The other two cases are when at 100 s into the simulation, prior to intracellular Ca^{2+} injection, $[Ca^{2+}]_{up}$ and $[Ca^{2+}]_{rel}$ were elevated and reduced to their values at 200% SERCA (bottom) and 20% SERCA (top) at 100 s respectively in the default case (see electronic supplementary material, figure S4A and B). The coloured crosses indicate where a change in the trend occurs in the corresponding case. SERCA, sarcoplasmic reticulum Ca^{2+}-ATPase; SD, spontaneous depolarization. (Online version in colour.)

were elevated to their values for 200% SERCA, the $[Ca^{2+}]_i$ SD threshold decreased relative to the threshold obtained in the default case for all values of SERCA. By contrast, when $[Ca^{2+}]_{rel}$ and $[Ca^{2+}]_{up}$ were reduced to their values for 20% SERCA, the $[Ca^{2+}]_i$ SD threshold instead increased relative to the threshold obtained in the default case for all values of SERCA.

4. Discussion

It is generally accepted that SDs/DADs are caused by spontaneous release of Ca^{2+} from the SR due to an upregulation in SERCA uptake and dysfunctional RyR in atrial cells [8,9]. However, recent mice knockout experiments of TBX5 have demonstrated that SDs could also occur through a reduced SERCA uptake, and increased I_{NaCa} and RyR [27,29,54]. Similar findings have also been reported in experimental and clinical studies of diabetes [6,31] and heart failure [30,32,33]. Surprisingly, in all these cases, the rescue of impaired SERCA uptake through the knockout of PLN or SERCA2a gene therapy was able to suppress these SDs [29,36–39]. To our knowledge, this is the first computational study that systematically investigates the sensitivity of SERCA in relation to other Ca^{2+} handling channels in the genesis of SDs/DADs and the mechanisms which are involved.

Though the results shown in this study are specific for the occurrence of SDs as they are easier to identify in simulations than DADs, the conclusions on the dynamic relationship between the key Ca^{2+} proteins, i.e. SERCA, I_{CaL}, I_{NaCa}, and RyR can be drawn similarly for DADs. Generally, in our simulations, DADs occur only in the form of a slight depolarization if changes to channels are close to the changes required to trigger an SD. For example, if we increased I_{CaL} to 112% of its control value instead (figure 3), then after the last stimulated AP, a self-depolarization up to −72 mV was observed. By contrast, at 113% of the control value of I_{CaL} and greater, SDs were observed.

Our four bifurcation analyses together illustrate that variations in SERCA can have a pronounced impact on Ca^{2+} handling. When SERCA is significantly inhibited (i.e. less than approx. 80% SERCA) or elevated (i.e. greater than approx. 100%), the minimum increase in RyR

or I_{CaL}, or decrease in I_{NaCa} that is required to trigger SDs is greater than when SERCA is only slightly inhibited (i.e. greater than approx. 80% SERCA and less than approx. 100% SERCA). This highlights that the myocyte's susceptibility to abnormal depolarizations is greatest when SERCA is slightly inhibited, because changes in RyR, I_{CaL}, and I_{NaCa} needed to trigger SDs/DADs in this parameter range for SERCA are at a minimum. These bifurcation diagrams also illustrate that increased RyR or I_{CaL} triggers SDs/DADs, but increased I_{NaCa} suppresses them instead. This is interesting, because in the setting of reduced TBX5, diabetes, and heart failure, SDs/DADs was observed alongside an elevation in I_{NaCa}. Therefore, for SDs/DADs to occur in conditions with an increased I_{NaCa}, there must also be an increase in I_{CaL} to overcome the suppression effects of I_{NaCa}.

In the dependency test by Fink *et al*., we found that in the full Maleckar *et al*. model, only the modulation of the RyR by $[Ca^{2+}]_i$ was crucial. This differs from the 37 previously published mathematical models of atrial and ventricular myocytes that they tested, where they found that in most models, it was the modulation of RyR through Ca^{2+} in the dyadic space ($[Ca^{2+}]_d$) that triggered SDs [40]. This could be because in most models they tested, the RyR is connected to the dyadic space rather than the intracellular space as is the case in the Maleckar *et al*. model.

During our experiment with intracellular Ca^{2+} injection protocol 1, we observed that diastolic $[Ca^{2+}]_{up}$ and $[Ca^{2+}]_{rel}$ at the time point where intracellular Ca^{2+} is injected to trigger spontaneous Ca^{2+} release decreased as SERCA decreased. This is consistent with experimental findings by Fernandez-Tenorio and Niggli, where they applied a range of pharmacological SERCA stimulators and a PLB antibody to mouse cardiomyocytes, and found that mice with non-stimulated SERCA had a lower diastolic $[Ca^{2+}]_{SR}$ prior to spontaneous Ca^{2+} release. Interestingly, they considered $[Ca^{2+}]_{SR}$ as being the threshold for spontaneous Ca^{2+} release, and this threshold increased as SERCA was elevated [61].

With the second intracellular Ca^{2+} injection protocol, we probed whether $[Ca^{2+}]_{up}$ and $[Ca^{2+}]_{rel}$ were indeed also factors in determining the $[Ca^{2+}]_i$ SD threshold. Results from this experiment revealed that in general, if $[Ca^{2+}]_{up}$ and $[Ca^{2+}]_{rel}$ are increased above their intrinsic value for a particular value of SERCA, then the $[Ca^{2+}]_i$ SD threshold will be lowered. However, if $[Ca^{2+}]_{up}$ and $[Ca^{2+}]_{rel}$ are decreased below their intrinsic value instead, then the $[Ca^{2+}]_i$ SD threshold will be elevated instead. From the point of view of this study, it is hence better to view $[Ca^{2+}]_{up}$ and $[Ca^{2+}]_{rel}$ alongside SERCA to be regulators of the $[Ca^{2+}]_i$ SD threshold rather than act as a threshold itself for spontaneous Ca^{2+} release and hence SDs/DADs as proposed by Fernandez-Tenorio and Niggli.

On closer inspection, this experiment also provides some insights into why the $[Ca^{2+}]_i$ SD threshold increases when SERCA is significantly inhibited (i.e. less than approx. 80% SERCA) or elevated (i.e. greater than approx. 100% SERCA). To illustrate the former situation, we consider the default case starting at 80% of its control value of SERCA in figure 8. If we reduce SERCA from 80% to 60% of its control value, the $[Ca^{2+}]_i$ SD threshold will increase slightly (80% SERCA to 60% SERCA on the blue line). If at 60% SERCA, $[Ca^{2+}]_{up}$ and $[Ca^{2+}]_{rel}$ are artificially reduced below its intrinsic value, the increase in the $[Ca^{2+}]_i$ SD threshold from 80% SERCA to 60% will be much greater (80% SERCA on the blue line to 60% SERCA on the red line). However, if at 60% SERCA, $[Ca^{2+}]_{up}$ and $[Ca^{2+}]_{rel}$ are artificially elevated above its intrinsic value, the $[Ca^{2+}]_i$ SD threshold from 80% SERCA to 60% will instead decrease (80% SERCA on the blue line to 60% SERCA on the green line). This seems to illustrate that in the default case, the $[Ca^{2+}]_i$ SD threshold starts to increase at less than approximately 80% SERCA because the maximum SERCA uptake is no longer high enough to maintain $[Ca^{2+}]_{up}$ and $[Ca^{2+}]_{rel}$ at sufficient levels. As a result, greater $[Ca^{2+}]_i$ is required to compensate this for spontaneous Ca^{2+} release and subsequently SDs to occur. In a similar fashion, we can illustrate the latter situation. However, the key difference here is that raising $[Ca^{2+}]_{up}$ and $[Ca^{2+}]_{rel}$ has a negligible impact on the $[Ca^{2+}]_i$ SD threshold (160% SERCA on the blue line to 160% SERCA on the green line).

This latter situation likely occurs because of the properties of the bidirectional SERCA pump. If maximum SERCA uptake is elevated, then this would result in an increase of $[Ca^{2+}]_{up}$ and $[Ca^{2+}]_{rel}$. Because $[Ca^{2+}]_{up}$ and $[Ca^{2+}]_{rel}$ are now elevated, the reverse mode of the bidirectional

pump activates, reducing the net Ca^{2+} uptake into the SR by SERCA. Further increasing $[Ca^{2+}]_{up}$ and $[Ca^{2+}]_{rel}$ would therefore have a negligible effect on the net Ca^{2+} uptake into the SR by SERCA. In this situation, an elevation in $[Ca^{2+}]_i$ is required to reduce the reverse direction of SERCA and restore SERCA uptake function such that spontaneous Ca^{2+} release and hence SDs/DADs can occur. In electronic supplementary material, figure S7, we have demonstrated that by replacing the bidirectional SERCA pump in the Maleckar *et al*. model with the unidirectional SERCA pump in the CRN model and a generic leak in the uptake compartment (electronic supplemental materials, figure S6), the minimum multiplier for RyR and I_{CaL} to trigger at least one SD is significantly less than in the bidirectional case, and significantly greater for I_{NaCa} for elevated SERCA (greater than approx. 100% SERCA), illustrating that the $[Ca^{2+}]_i$ SD threshold is much lower with a unidirectional SERCA pump than a bidirectional one in this parameter range.

Based on these findings together, we therefore hypothesize that there are three main phases in the Ca^{2+} handling involving SERCA, $[Ca^{2+}]_{up}$, and $[Ca^{2+}]_{rel}$ which attribute to the $[Ca^{2+}]_i$ SD threshold in the full Maleckar *et al*. model at varying levels of maximum SERCA uptake. If SERCA is significantly inhibited (i.e. less than approx. 80% SERCA), the bidirectional SERCA pump becomes too inhibited to uptake enough calcium into the SR necessary to aid in the initiation of spontaneous Ca^{2+} release and hence SDs, and so an elevation in $[Ca^{2+}]_i$ is required to compensate (figure 9*a*).

On the other hand, when SERCA is elevated (e.g. PLN knockout or SERCA2a gene therapy) (i.e. greater than approx. 100% SERCA), the properties of the bidirectional SERCA pump becomes pronounced. The resultant $[Ca^{2+}]_{up}$ and $[Ca^{2+}]_{rel}$ become relatively high, which trigger the reverse direction of the pump. This in turn reduces the net uptake of Ca^{2+} into the SR and disrupts the ability of SERCA to contribute to spontaneous Ca^{2+} release and hence SDs. To promote the forward direction of the bidirectional SERCA pump in this situation, there needs to be an increase in $[Ca^{2+}]_i$ such that $[Ca^{2+}]_{up}$ and $[Ca^{2+}]_{rel}$ do not appear relatively high (figure 9*c*).

Figure 9*b* illustrates when SERCA is in the ideal range to trigger SDs (i.e. greater than approx. 80% SERCA and less than approx. 100% SERCA). In this range, SERCA has sufficient uptake into the SR such that $[Ca^{2+}]_{up}$ and $[Ca^{2+}]_{rel}$ reach appropriate levels without triggering the reverse mode of the SERCA pump and without a compensatory increase in $[Ca^{2+}]_i$. As a result, the $[Ca^{2+}]_i$ SD threshold is at a minimal in this range, and only small increases in RyR and I_{CaL}, or decreases in I_{NaCa} are required.

5. Limitations

There are several limitations to this modelling study. The first issue concerns the insufficient details of spatial Ca^{2+} handling in the Maleckar *et al*. model. The internal structure of Ca^{2+} handling in cardiac myocytes is vastly more complicated than is represented in common pool models. The SR is a complex structural network within the myocyte and consists of clusters of RyRs which can open and close collectively. To be able to expand the scope of this study to include the mechanisms by which a modulation of SERCA can increase the incidence and spatial dynamics of Ca^{2+} waves, and how normalization or elevation of SERCA can reduce this, the descriptions of Ca^{2+} handling in the Maleckar *et al*. model need to be further developed to include these structural and spatial aspects of Ca^{2+} handling, such as the Voigt *et al*. [7] and Thul *et al*. models [62,63]. Additionally, the peak systolic $[Ca^{2+}]_i$ level and decay of $[Ca^{2+}]_i$ in our simulated results of the Maleckar *et al*. model are different from those in the experimental studies by Neef *et al*. and Voigt *et al*. [7,64,65]. This is because the Maleckar *et al*. model was based on the Nygren *et al*. model, which was validated through a different experimental study on human atrial myocytes. Further investigation is required to ascertain the modifications which are required in the formulations of the ionic and Ca^{2+} handling channels such that the model can accurately capture the experimental results by Neef *et al*. and Voigt *et al*. as well as the phenomena in SERCA as detailed in this study.

Limited availability of data for SERCA and other Ca^{2+} handling channels in the setting of reduced TBX5, diabetes, and heart failure is also an obstacle of this study. Across these settings,

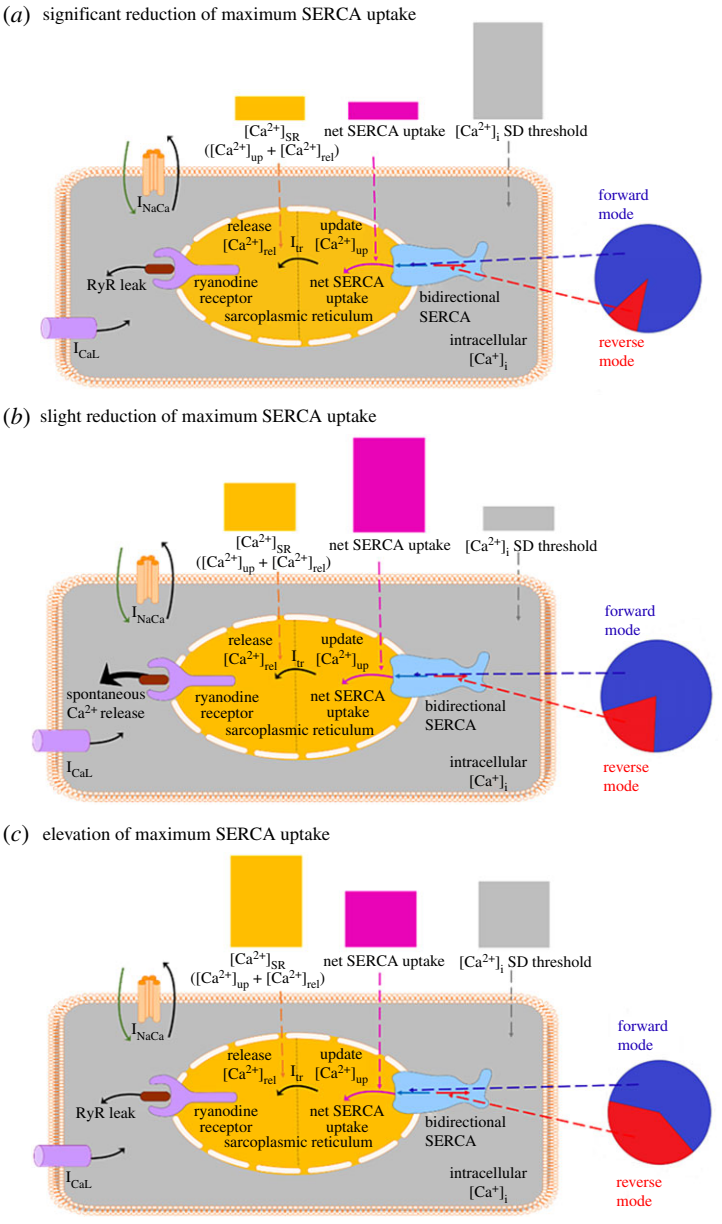

Figure 9. Schematic illustrating the general differences in Ca^{2+} handling for maximum SERCA uptake ranges between (*a*) approximately 20–80% (*b*) approximately 80–100% and (*c*) greater than approximately 100% of its control value in the Maleckar *et al*. model. Pie graph inserts show the relative magnitude of the forward and reverse mode of the bidirectional SERCA pump in each range. Bar graph inserts qualitatively highlight the relative magnitude of the net SERCA uptake and $[Ca^{2+}]_{SR}$ in each range, and how this impacts the magnitude of the $[Ca^{2+}]_i$ threshold for SDs. SERCA, sarcoplasmic reticulum Ca^{2+}-ATPase; SD, spontaneous depolarization. (Online version in colour.)

studies only provide the voltage-clamp recordings of I_{CaL} and caffeine-based protocol results of SERCA and I_{NaCa} for a select few myocytes [6,29,54,55,66], and so it would be difficult to verify if any parameters that we assigned would fall under physiological ranges. In our study, we instead conducted a modelling analysis of how changes in the conductivity of I_{CaL}, I_{NaCa}, and RyR, and the uptake of SERCA impacts Ca^{2+} handling in the atrial myocyte across a wide parameter space

to qualitatively examine the mechanisms by which a reduction in SERCA can trigger SDs, and how normalization or elevation of SERCA through knockout of PLN or SERCA2a gene therapy can suppress SDs.

While this approach provides insights as to how Ca^{2+} handling is altered as we vary maximum SERCA uptake and the relationships between SERCA and other Ca^{2+} handling channels in triggering SDs, it can only make predictions into the physiological ranges where these phenomena can occur. This may be where it would be more advantageous to use a population-based approach combined with a complementary animal study [67] to investigate if deviations from the limited data that we have on Ca^{2+} handling channels under reduced TBX5, diabetes, and heart failure can still give rise to SDs, and for a better estimate of the parameter ranges where SDs can be triggered or suppressed. Experimental studies in reduced TBX5, diabetes, and heart failure used varying experimental and pacing protocols [6,27,29,54,55,66]. In our simulations with the Maleckar *et al*. model, a pacing frequency of 1 Hz was used instead as we are interested in how reduced SERCA impacts Ca^{2+} handling to trigger SDs, and how normalization or elevation of SERCA can suppress SDs in human atrial myocytes. While we currently lack the experimental data to verify our results, it would, however, be of benefit to this study if simulations were conducted at multiple different pacing frequencies. This could be because changing the pacing frequency would likely also affect $[Ca^{2+}]_{up}$ and $[Ca^{2+}]_{rel}$, causing an increase in the $[Ca^{2+}]_i$ SD threshold.

In terms of the suppression of SDs due to the knockout of PLN, this was regarded as an increase in maximum SERCA uptake back to normal or elevated levels. This is analogous to changing the maximum conductance through agents such as a pharmacological inhibitor or through SERCA2a gene therapy. However, disruption of PLN-mediated SERCA inhibition can also cause an increased affinity to $[Ca^{2+}]_i$ and therefore likely shift the balance between the forward and reverse mode of SERCA. Hence for our hypothesis to hold, it is assumed that changes in SERCA activity are exclusive to changes in its maximum SERCA uptake. Disruption of PLN-mediated SERCA inhibition could be more rigorously modelled as changes in the phosphorylation rates of SERCA and could potentially shed more insight into the Ca^{2+} handling mechanisms attributing to the suppression of SDs/DADs if these parameters were also investigated through a bifurcation analysis and intracellular Ca^{2+} injection protocol to gauge how changes in phosphorylation rates impacted the $[Ca^{2+}]_i$ threshold. Similarly, the impact of Ca^{2+} buffering on Ca^{2+} handling warrants investigation through these analytical methods.

The second caveat in our hypothesis is that for spontaneous Ca^{2+} release to occur, there must also be sufficient diffusion of Ca^{2+} in the SR. Diffusion of Ca^{2+} through the SR has been shown to be a critical factor of spontaneous Ca^{2+} release in atrial myocytes [68]. Rapid Ca^{2+} diffusion within the SR is necessary to stabilize and balance $[Ca^{2+}]_{SR}$ within the myocyte. In the context of this study, reducing Ca^{2+} diffusion could potentially cause an overall reduction in $[Ca^{2+}]_{up}$ and $[Ca^{2+}]_{rel}$, which subsequently increases the $[Ca^{2+}]_i$ SD threshold.

The other intermediate pathway that was not considered in the Maleckar *et al*. model or in our mathematical analyses was the Ca^{2+}/calmodulin-dependent protein kinase II (CaMKII). A reduction in SERCA uptake would increase diastolic $[Ca^{2+}]_i$, and thus lead to greater phosphorylation of PLN on SERCA or RyR. This in turn could mitigate the reduced SERCA uptake and increase the open probability of RyR and could potentially also explain the onset of SDs from a reduced SERCA, and the suppression of SDs from PLN knockout or SERCA2a gene therapy [69]. More recently, Alsina *et al*. discovered an intermediate pathway involving a novel protein phosphatase 1 (PP1)- regulatory subunit PPP1R3A (PP1 regulatory subunit type 3A) within the RyR2 channel complex. Through the knockout of PPP1R3A, they demonstrated that reduced expression of this novel PP1 regulatory subunit reduces the binding of PP1 to both RyR2 and PLN, which subsequently increases SR Ca^{2+} release and hence increases the susceptibility of the myocyte to SDs [70]. Changes in Ca^{2+} handling channels can therefore have an impact on the dynamics of this intermediate pathway and thus the $[Ca^{2+}]_i$ SD threshold, and would need to be incorporated along with the intermediate pathway involving CaMKII in a future study.

6. Conclusion

In summary, a reduction in SERCA alone cannot cause SDs/DADs, but instead affects the $[Ca^{2+}]_i$ threshold required to trigger SDs/DADs. Compensatory changes in other Ca^{2+} handling channels, such as increasing RyR/ I_{CaL} or decreasing I_{NaCa} alongside SERCA are therefore required to raise $[Ca^{2+}]_i$ to its threshold level to trigger spontaneous Ca^{2+} release and hence SDs/DADs. Furthermore, this study also demonstrates that a bidirectional SERCA pump is necessary to capture the effects of SD/DAD initiation particularly due to a reduction in SERCA and $[Ca^{2+}]_{SR}$ load. For the first time, our modelling study reconciles different mechanisms of abnormal depolarizations in the setting of 'lone' AF, TBX5, diabetes, and heart failure, and it may lead to more targeted treatment for these patients, such as the suppression of SDs/DADs from the normalization or elevation of SERCA from PLN knockout or SERCA2a gene therapy.

Data accessibility. All supporting data and computer simulation source code can be accessed at the CELLML depository (https://models.physiomeproject.org/exposure/bbd802c6a6d6e69b746244f83b4fb89b/maleckar_greenstein_trayanova_giles_2009.cellml) and the GitHub repository (https://github.com/SirAndii/AndyHub/blob/master/MaleckarCaSubsystemControl.m).

Authors' contributions. A.L. and J.Z. conceived and designed the study. A.L. conducted the experiments and drafted the manuscript. A.L., J.B., P.A.G., V.V.F. and J.Z. interpreted the data, and reviewed, revised and approved the final version of this manuscript.

Competing interests. The authors have no competing interests.

Funding. This work was supported by the Health Research Council of New Zealand (16/385), the National Institutes of Health grant nos (HL115580 and HL135109), the National Natural Science Foundation of China (grant no. 61901192) and the National Key R&D Program of China (grant nos 2019YFC0120100 and 2019YFC0121900).

References

1. Feghaly J, Zakka P, London B, MacRae CA, Refaat MM. 2018 Genetics of atrial fibrillation. *J. Am. Heart Assoc.* **7**, e009884. (doi:10.1161/JAHA.118.009884)
2. Benjamin EJ, Chen P-S, Bild DE, Mascette AM, Albert CM, Alonso A *et al.* 2009 Prevention of atrial fibrillation: report from a national heart, lung, and blood institute workshop. *Circulation* **119**, 606–618. (doi:10.1161/CIRCULATIONAHA.108.825380)
3. Magnani JW, Hylek EM, Apovian CM. 2013 Obesity begets atrial fibrillation: a contemporary summary. *Circulation* **128**, 401–405. (doi:10.1161/CIRCULATIONAHA.113.001840)
4. Asghar O, Alam U, Hayat SA, Aghamohammadzadeh R, Heagerty AM, Malik RA. 2012 Obesity, diabetes and atrial fibrillation; epidemiology, mechanisms and interventions. *Curr. Cardiol. Rev.* **8**, 253–264. (doi:10.2174/157340312803760749)
5. Wasmer K, Eckardt L, Breithardt G. 2017 Predisposing factors for atrial fibrillation in the elderly. *J. Geriatr. Cardiol. JGC.* **14**, 179.
6. Hamilton S, Terentyev D. 2018 Proarrhythmic remodeling of calcium homeostasis in cardiac disease; implications for diabetes and obesity. *Front. Physiol.* **9**, 1517. (doi:10.3389/fphys.2018.01517)
7. Voigt N, Heijman J, Wang Q, Chiang DY, Li N, Karck M, Wehrens XH, Nattel S, Dobrev D. 2014 Cellular and molecular mechanisms of atrial arrhythmogenesis in patients with paroxysmal atrial fibrillation. *Circulation* **129**, 145–156. (doi:10.1161/CIRCULATIONAHA.113.006641)
8. Iwasaki Y-k, Nishida K, Kato T, Nattel S. 2011 Atrial fibrillation pathophysiology: implications for management. *Circulation* **124**, 2264–2274. (doi:10.1161/CIRCULATIONAHA.111.019893)
9. Nattel S, Burstein B, Dobrev D. 2008 Atrial remodeling and atrial fibrillation: mechanisms and implications. *Circ. Arrhythmia Electrophysiol.* **1**, 62–73. (doi:10.1161/CIRCEP.107.754564)
10. Shanmugam M, Molina CE, Gao S, Severac-Bastide R, Fischmeister R, Babu GJ. 2011 Decreased sarcolipin protein expression and enhanced sarco (endo) plasmic reticulum Ca^{2+} uptake in human atrial fibrillation. *Biochem. Biophys. Res. Commun.* **410**, 97–101. (doi:10.1016/j.bbrc.2011.05.113)
11. Potpara TS, Lip GYH. 2015 A brief history of 'lone' atrial fibrillation: from 'a peculiar pulse irregularity' to a modern public health concern. *Curr. Pharm. Des.* **21**, 679–696. (doi:10.2174/1381612820666140929100209)

12. Fox CS, Parise H, D'Agostino Sr RB, Lloyd-Jones DM, Vasan RS, Wang TJ, Levy D, Wolf PA, Benjamin EJ. 2004 Parental atrial fibrillation as a risk factor for atrial fibrillation in offspring. *JAMA* **291**, 2851–2855. (doi:10.1001/jama.291.23.2851)
13. Ellinor PT, Yoerger DM, Ruskin JN, MacRae CA. 2005 Familial aggregation in lone atrial fibrillation. *Hum. Genet.* **118**, 179–184. (doi:10.1007/s00439-005-0034-8)
14. Arnar DO, Thorvaldsson S, Manolio TA, Thorgeirsson G, Kristjansson K, Hakonarson H, Stefansson K. 2006 Familial aggregation of atrial fibrillation in Iceland. *Eur. Heart J.* **27**, 708–712. (doi:10.1093/eurheartj/ehi727)
15. Øyen N, Ranthe MF, Carstensen L, Boyd HA, Olesen MS, Olesen S-P, Wohlfahrt J, Melbye M. 2012 Familial aggregation of lone atrial fibrillation in young persons. *J. Am. Coll. Cardiol.* **60**, 917–921. (doi:10.1016/j.jacc.2012.03.046)
16. Marcus GM, Smith LM, Vittinghoff E, Tseng ZH, Badhwar N, Lee BK, Lee RJ, Scheinman MM, Olgin JE. 2008 A first-degree family history in lone atrial fibrillation patients. *Heart Rhythm* **5**, 826–830. (doi:10.1016/j.hrthm.2008.02.016)
17. Mahida S. 2014 Genetic discoveries in atrial fibrillation and implications for clinical practice. *ArrhythmiaElectrophysiol. Rev.* **3**, 69. (doi:10.15420/aer.2014.3.2.69)
18. Hucker WJ, Saini H, Lubitz SA, Ellinor PT. 2016 Atrial fibrillation genetics: is there a practical clinical value now or in the future? *Can. J. Cardiol.* **32**, 1300–1305. (doi:10.1016/j.cjca.2016.02.032)
19. Kalstø SM, Siland JE, Rienstra M, Christophersen IE. 2019 Atrial fibrillation genetics update: towards clinical implementation. *Front. Cardiovasc. Med.* **6**, 127. (doi:10.3389/fcvm.2019.00127)
20. Zang X *et al.* 2013 SNP rs3825214 in TBX5 is associated with lone atrial fibrillation in Chinese Han population. *PLoS ONE* **8**, e64966. (doi:10.1371/journal.pone.0064966)
21. Christophersen IE *et al.* 2017 Fifteen genetic loci associated with the electrocardiographic P wave. *Circ. Cardiovas. Genet.* **10**, e001667. (doi:10.1161/CIRCGENETICS.116.001667)
22. Tucker NR, Ellinor PT. 2014 Emerging directions in the genetics of atrial fibrillation. *Circ. Res.* **114**, 1469–1482. (doi:10.1161/CIRCRESAHA.114.302225)
23. Mahida S, Ellinor PT. 2012 New advances in the genetic basis of atrial fibrillation. *J. Cardiovasc. Electrophysiol.* **23**, 1400–1406. (doi:10.1111/j.1540-8167.2012.02445.x)
24. Holm H *et al.* 2010 Several common variants modulate heart rate, PR interval and QRS duration. *Nat. Genet.* **42**, 117. (doi:10.1038/ng.511)
25. Garg V *et al.* 2003 GATA4 mutations cause human congenital heart defects and reveal an interaction with TBX5. *Nature* **424**, 443. (doi:10.1038/nature01827)
26. Guo DF *et al.* 2016 TBX5 loss-of-function mutation contributes to atrial fibrillation and atypical Holt-Oram syndrome. *Mol. Med. Rep.* **13**, 4349–4356. (doi:10.3892/mmr.2016.5043)
27. Nadadur RD *et al.* 2016 Pitx2 modulates a Tbx5-dependent gene regulatory network to maintain atrial rhythm. *Sci. Trans. Med.* **8**, 354ra115. (doi:10.1126/scitranslmed.aaf4891)
28. Antzelevitch C, Burashnikov A. 2011 Overview of basic mechanisms of cardiac arrhythmia. *Cardiac. Electrophysiol. Clin.* **3**, 23–45. (doi:10.1016/j.ccep.2010.10.012)
29. Dai W *et al.* 2019 A calcium transport mechanism for atrial fibrillation in Tbx5-mutant mice. *eLife* **8**, e41814. (doi:10.7554/eLife.41814)
30. Marks AR. 2013 Calcium cycling proteins and heart failure: mechanisms and therapeutics. *J. Clin. Invest.* **123**, 46–52. (doi:10.1172/JCI62834)
31. Lacombe VA, Viatchenko-Karpinski S, Terentyev D, Sridhar A, Emani S, Bonagura JD, Feldman DS, Gyorke S, Carnes CA. 2007 Mechanisms of impaired calcium handling underlying subclinical diastolic dysfunction in diabetes. *Am. J. Physiol. Regul., Integr. Comp. Physiol.* **293**, R1787–R1797. (doi:10.1152/ajpregu.00059.2007)
32. Priebe L, Beuckelmann DJ. 1998 Simulation study of cellular electric properties in heart failure. *Circ. Res.* **82**, 1206–1223. (doi:10.1161/01.RES.82.11.1206)
33. Bers DM, Eisner DA, Valdivia HH. 2003 Sarcoplasmic reticulum Ca^{2+} and heart failure: roles of diastolic leak and Ca^{2+} transport. *Am. Heart Assoc.*
34. Popescu I, Yin G, Velmurugan S, Erickson JR, Despa F, Despa S. 2019 Lower sarcoplasmic reticulum Ca^{2+} threshold for triggering afterdepolarizations in diabetic rat hearts. *Heart Rhythm* **16**, 765–772. (doi:10.1016/j.hrthm.2018.11.001)
35. Verkerk AO, Veldkamp MW, Baartscheer A, Schumacher CA, Klöpping C, van Ginneken AC, Ravesloot JH. 2001 Ionic mechanism of delayed afterdepolarizations in

ventricular cells isolated from human end-stage failing hearts. *Circulation* **104**, 2728–2733. (doi:10.1161/hc4701.099577)
36. Shanmugam M, Gao S, Hong C, Fefelova N, Nowycky MC, Xie L-H, Periasamy M, Babu GJ. 2010 Ablation of phospholamban and sarcolipin results in cardiac hypertrophy and decreased cardiac contractility. *Cardiovasc. Res.* **89**, 353–361. (doi:10.1093/cvr/cvq294)
37. Karakikes I, Kim M, Hadri L, Sakata S, Sun Y, Zhang W, Chemaly ER, Hajjar RJ, Lebeche D. 2009 Gene remodeling in type 2 diabetic cardiomyopathy and its phenotypic rescue with SERCA2a. *PLoS ONE* **4**, e6474. (doi:10.1371/journal.pone.0006474)
38. Lyon AR *et al.* 2011 SERCA2a gene transfer decreases sarcoplasmic reticulum calcium leak and reduces ventricular arrhythmias in a model of chronic heart failure. *Circ. Arrhythmia Electrophysiol.* **4**, 362–372. (doi:10.1161/CIRCEP.110.961615)
39. Roe AT, Frisk M, Louch WE. 2015 Targeting cardiomyocyte Ca^{2+} homeostasis in heart failure. *Curr. Pharm. Des* **21**, 431–448. (doi:10.2174/1381612821041412041241 29)
40. Fink M, Noble PJ, Noble D. 2011 Ca2+-induced delayed afterdepolarizations are triggered by dyadic subspace Ca^{2+} affirming that increasing SERCA reduces aftercontractions. *Am. J. Physiol. Heart Circ. Physiol.* **301**, H921–HH35. (doi:10.1152/ajpheart.01055.2010)
41. January CT, Fozzard H. 1988 Delayed afterdepolarizations in heart muscle: mechanisms and relevance. *Pharmacol. Rev.* **40**, 219–227.
42. Jiang D, Xiao B, Yang D, Wang R, Choi P, Zhang L, Cheng H, Chen SRW. 2004 RyR2 mutations linked to ventricular tachycardia and sudden death reduce the threshold for store-overload-induced Ca^{2+} release (SOICR). *Proc. Natl Acad. Sci. USA.* **101**, 13 062–13 067. (doi:10.1073/pnas.0402388101)
43. Jiang D, Wang R, Xiao B, Kong H, Hunt DJ, Choi P, Zhang L, Chen SRW. 2005 Enhanced store overload–induced Ca^{2+} release and channel sensitivity to luminal Ca^{2+} activation are common defects of RyR2 mutations linked to ventricular tachycardia and sudden death. *Circ. Res.* **97**, 1173–1181. (doi:10.1161/01.RES.0000192146.85173.4b)
44. Tweedie D, Harding SE, MacLeod KT. 2000 Sarcoplasmic reticulum Ca^{2+} content, sarcolemmal Ca^{2+} influx and the genesis of arrhythmias in isolated guinea-pig cardiomyocytes. *J. Mol. Cell. Cardiol.* **32**, 261–272. (doi:10.1006/jmcc.1999.1070)
45. Louch WE *et al.* 2010 Sodium accumulation promotes diastolic dysfunction in end-stage heart failure following Serca2 knockout. *J. Physiol.* **588**, 465–478. (doi:10.1113/jphysiol.2009.183517)
46. Andersson KB *et al.* 2009 Moderate heart dysfunction in mice with inducible cardiomyocyte-specific excision of the Serca2 gene. *J. Mol. Cell. Cardiol.* **47**, 180–187. (doi:10.1016/j.yjmcc.2009.03.013)
47. Li L, Louch WE, Niederer SA, Aronsen JM, Christensen G, Sejersted OM, Smith NÂP. 2012 Sodium accumulation in SERCA knockout-induced heart failure. *Biophys. J.* **102**, 2039–2048. (doi:10.1016/j.bpj.2012.03.045)
48. Bai J, Gladding PA, Stiles MK, Fedorov VV, Zhao J. 2018 Ionic and cellular mechanisms underlying TBX5/PITX2 insufficiency-induced atrial fibrillation: insights from mathematical models of human atrial cells. *Sci. Rep.* **8**, 15642. (doi:10.1038/s41598-018-33958-y)
49. Maleckar MM, Greenstein JL, Trayanova NA, Giles WR. 2008 Mathematical simulations of ligand-gated and cell-type specific effects on the action potential of human atrium. *Prog. Biophys. Mol. Biol.* **98**, 161–170. (doi:10.1016/j.pbiomolbio.2009.01.010)
50. Nygren A, Fiset C, Firek L, Clark JW, Lindblad DS, Clark RB, Giles WR. 1998 Mathematical model of an adult human atrial cell: the role of K^+ currents in repolarization. *Circ. Res.* **82**, 63–81. (doi:10.1161/01.RES.82.1.63)
51. Nygren A, Leon L, Giles W. 2001 Simulations of the human atrial action potential. *Phil. Trans. R. Soc. A* **359**, 1111–1125. (doi:10.1098/rsta.2001.0819)
52. Wilhelms M, Hettmann H, Maleckar MMC, Koivumäki JT, Dössel O, Seemann G. 2013 Benchmarking electrophysiological models of human atrial myocytes. *Front. Physiol.* **3**, 487. (doi:10.3389/fphys.2012.00487)
53. Koivumäki JT, Takalo J, Korhonen T, Tavi P, Weckström M. 2009 Modelling sarcoplasmic reticulum calcium ATPase and its regulation in cardiac myocytes. *Phil. Trans. R. Soc. A* **367**, 2181–2202. (doi:10.1098/rsta.2008.0304)
54. Laforest B, Dai W, Tyan L, Lazarevic S, Shen KM, Gadek M, Broman MT, Weber CR, Moskowitz IP. 2019 Atrial fibrillation risk loci interact to modulate Ca^{2+}-dependent atrial rhythm homeostasis. *J. Clin. Invest.***129**, 4937–4950. (doi:10.1172/JCI124231)

55. Pogwizd SM, Schlotthauer K, Li L, Yuan W, Bers DM. 2001 Arrhythmogenesis and contractile dysfunction in heart failure: roles of sodium-calcium exchange, inward rectifier potassium current, and residual β-adrenergic responsiveness. *Circ. Res.* **88**, 1159–1167. (doi:10.1161/hh1101.091193)
56. Stambler BS, Fenelon G, Shepard RK, Clemo HF, Guiraudon CM. 2003 Characterization of sustained atrial tachycardia in dogs with rapid ventricular pacing-induced heart failure. *J. Cardiovasc. Electrophysiol.* **14**, 499–507. (doi:10.1046/j.1540-8167.2003.02519.x)
57. Rizzi N *et al.* 2008 Unexpected structural and functional consequences of the R33Q homozygous mutation in cardiac calsequestrin: a complex arrhythmogenic cascade in a knock in mouse model. *Circ. Res.* **103**, 298–306. (doi:10.1161/CIRCRESAHA.108.171660)
58. Song Y, Shryock JC, Belardinelli L. 2008 An increase of late sodium current induces delayed afterdepolarizations and sustained triggered activity in atrial myocytes. *Am. J. Physiol. Heart Circ. Physiol.* **294**, H2031–H20H9. (doi:10.1152/ajpheart.01357.2007)
59. Marban E, Robinson SW, Wier WG. 1986 Mechanisms of arrhythmogenic delayed and early afterdepolarizations in ferret ventricular muscle. *J. Clin. Invest.* **78**, 1185–1192. (doi:10.1172/JCI112701)
60. Kass RS, Tsien RW. 1982 Fluctuations in membrane current driven by intracellular calcium in cardiac Purkinje fibers. *Biophys. J.* **38**, 259–269. (doi:10.1016/S0006-3495(82)84557-8)
61. Fernandez-Tenorio M, Niggli E. 2018 Stabilization of Ca^{2+} signaling in cardiac muscle by stimulation of SERCA. *J. Mol. Cell. Cardiol.* **119**, 87–95. (doi:10.1016/j.yjmcc.2018.04.015)
62. Thul R, Coombe S, Roderick HL, Bootman MD. 2012 Subcellular calcium dynamics in a whole-cell model of an atrial myocyte. *Proc. Natl Acad. Sci. USA* **109**, 2150–2155. (doi:10.1073/pnas.1115855109)
63. Marchena M, Echebarria B. 2018 Computational model of calcium signaling in cardiac atrial cells at the submicron scale. *Front. Physiol.* **9**, 1760. (doi:10.3389/fphys.2018.01760)
64. Neef S *et al.* 2010 Novelty and significance. *Circ. Res.* **106**, 1134–1144. (doi:10.1161/CIRCRESAHA.109.203836)
65. Voigt N *et al.* 2012 Enhanced sarcoplasmic reticulum Ca^{2+} leak and increased Na^{+}-Ca^{2+} exchanger function underlie delayed afterdepolarizations in patients with chronic atrial fibrillation. *Circulation* **125**, 2059–2070. (doi:10.1161/CIRCULATIONAHA.111.067306)
66. Puglisi JL, Bers DM. 2001 LabHEART: an interactive computer model of rabbit ventricular myocyte ion channels and Ca transport. *Am. J. Physiol. Cell Physiol.* **281**, C2049–C2C60. (doi:10.1152/ajpcell.2001.281.6.C2049)
67. Devenyi RA, Sobie EA. 2016 There and back again: iterating between population-based modeling and experiments reveals surprising regulation of calcium transients in rat cardiac myocytes. *J. Mol. Cell. Cardiol.* **96**, 38–48. (doi:10.1016/j.yjmcc.2015.07.016)
68. Bers DM, Shannon TR. 2013 Calcium movements inside the sarcoplasmic reticulum of cardiac myocytes. *J. Mol. Cell. Cardiol.* **58**, 59–66. (doi:10.1016/j.yjmcc.2013.01.002)
69. Louch WE, Stokke MK, Sjaastad I, Christensen G, Sejersted OM. 2012 No rest for the weary: diastolic calcium homeostasis in the normal and failing myocardium. *Physiology* **27**, 308–323. (doi:10.1152/physiol.00021.2012)
70. Alsina KM *et al.* 2019 Loss of protein phosphatase 1 regulatory subunit PPP1R3A promotes atrial fibrillation. *Circulation* **140**, 681–693. (doi:10.1161/CIRCULATIONAHA.119.039642)